AGU PUBLICATIONS

Geophysical Research Letters

RESEARCH LETTER
10.1002/2014GL062759

Key Points:
- Large amounts of Pacific freshwater were found in the EGC between 2011 and 2013
- The maximum of Pacific water in 2013 was as large as last seen in 1998
- Thirty percent of the freshwater flux in the EGC in 2013 consisted of Pacific freshwater

Correspondence to:
L. de Steur,
Laura.de.Steur@nioz.nl

Citation:
de Steur, L., R. S. Pickart, D. J. Torres, and H. Valdimarsson (2015), Recent changes in the freshwater composition east of Greenland, *Geophys. Res. Lett.*, *42*, 2326–2332, doi:10.1002/2014GL062759.

Received 15 DEC 2014
Accepted 4 MAR 2015
Accepted article online 10 MAR 2015
Published online 1 APR 2015

Recent changes in the freshwater composition east of Greenland

L. de Steur[1,2], R. S. Pickart[3], D. J. Torres[3], and H. Valdimarsson[4]

[1]Royal Netherlands Institute for Sea Research, Texel, Netherlands, [2]Norwegian Polar Institute, Tromsø, Norway, [3]Woods Hole Oceanographic Institution, Woods Hole, Massachusetts, USA, [4]Marine Research Institute, Reykjavik, Iceland

Abstract Results from three hydrographic surveys across the East Greenland Current between 2011 and 2013 are presented with focus on the freshwater sources. End-member analysis using salinity, $\delta^{18}O$, and nutrient data shows that while meteoric water dominated the freshwater content, a significant amount of Pacific freshwater was present near Denmark Strait with a maximum in August 2013. While in 2011 and 2012 the net sea ice melt was dominated by brine, in 2013 it became close to zero. The amount of Pacific freshwater observed near Denmark Strait in 2013 is as large as the previous maximum in 1998. This, together with the decrease in meteoric water and brine, suggests a larger contribution from the Canadian Basin. We hypothesize that the increase of Pacific freshwater is the result of enhanced flux through Bering Strait and a shorter pathway of Pacific water through the interior Arctic to Fram Strait.

1. Introduction

Freshwater in the upper layer of the Arctic Ocean has increased significantly during the last decade [*Giles et al.*, 2012; *Morison et al.*, 2012]. Enhanced amounts of freshwater have been observed in the Beaufort Gyre since 2003 [*Proshutinsky et al.*, 2009], and a total of 8400 km^3 of freshwater had accumulated in the Arctic between the 1990s and 2008 [*Rabe et al.*, 2011]. Between 2007 and 2011 a fresh anomaly was observed to pass through the Lincoln Sea, north of Greenland, likely exiting the Arctic through Fram Strait and/or Nares Strait [*de Steur et al.*, 2013]. An anomalous release of freshwater from the Arctic into the Nordic Seas or subpolar Atlantic could modify stratification and inhibit vertical mixing, with possible consequences for dense water formation [*Dickson et al.*, 2007]. Arctic freshwater derives mainly from three sources: meteoric water (MW), Pacific water (PW), and sea ice melt (SIM) [*Bauch et al.*, 1995; *Jones et al.*, 1998]. Of these sources, MW (composed roughly of two thirds Siberian river water and one third net precipitation) is the largest contributor [see, e.g., *Serreze et al.*, 2006]. Low-salinity PW enters the Arctic through Bering Strait and is found mostly in the Canada Basin but is also advected across the Arctic with the Transpolar Drift Stream depending on the atmospheric circulation [*Steele et al.*, 2004]. Apart from summer meltwater found at the surface, SIM in the Arctic has generally been negative since brine input associated with freezing dominates over melting [*Aagaard et al.*, 1985].

The recent increase of freshwater in the central Arctic has been attributed mainly to an accumulation of MW [*Morison et al.*, 2012]. However, the inflow through Bering Strait has increased by 50% between 2001 and 2011 [*Woodgate et al.*, 2012], and Arctic sea ice cover has continued to decline since 1979, with a record minimum in 2012 [*Perovich et al.*, 2012]. In Fram Strait, through which the largest export of Arctic liquid freshwater takes place, indicators of Arctic change have also been observed. Since 2009, positive SIM fractions have been found and Pacific water was again observed in 2011 [*Dodd et al.*, 2012], after having been absent since the late 1990s [*Falck et al.*, 2005]. In addition, a significant reduction of sea ice thickness has been observed, most notably since 2006 [*Hansen et al.*, 2013]. Here we investigate the sources and the southward progression of Arctic freshwater found on sections that cross the East Greenland Current (EGC) and extend into the basin, between Denmark Strait and Fram Strait. The composition of the freshwater is established using an end-member analysis of recently collected shipboard data. Particular attention is given to a section across the EGC roughly 350 km north of Denmark Strait, known as the Kögur section, for which data are available from 2011, 2012, and 2013. These observations are then compared to earlier measurements from the 1990s and mid-2000s.

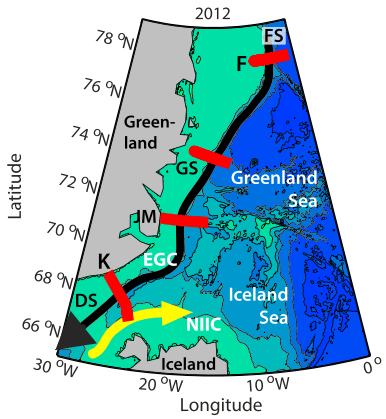

Figure 1. Map of the study region showing the hydrographic sections Kögur (K), Jan Mayen (JM), Greenland Sea (GS), and Fram (F) occupied in August 2012 between Denmark Strait (DS) and Fram Strait (FS). The East Greenland Current (EGC) and North Icelandic Irminger Current (NIIC) are shown with black and yellow arrows, respectively. Bathymetric contours are shown every 700 m.

2. Data and Methods

Most of the hydrographic, tracer, and velocity data used in the study come from four sections occupied by RRS James Clark Ross from 28 July to 25 August 2012, between the Denmark and Fram Straits (Figure 1). The sections are referred to as K (Kögur), JM (Jan Mayen), GS (Greenland Sea), and F (Fram Strait). All of the transects crossed the shelf break EGC but had variable coverage on the shelf and into the basin. Data from section K were also obtained in late August 2011 (R/V *Knorr*) and in early August 2013 (R/V *Bjarni Sæmundsson*). Only in 2012 did section K extend far enough to sample the northward flowing North Icelandic Irminger Current (NIIC). In 2012 sea ice was present on section GS (moderate ice cover) and on section F (heavy ice cover). Section K was ice free in all years.

The salinity (S) and temperature (T) data were collected with a Sea-Bird 911+ conductivity-temperature-depth (CTD) system and averaged into 2 db bins. Freshwater content (FWC) was determined as $\mathrm{FWC} = \int (S_{\mathrm{ref}} - S)/S_{\mathrm{ref}} \cdot dz$, relative to a reference salinity $S_{\mathrm{ref}} = 34.9$, the mean salinity in Fram Strait [*Holfort et al.*, 2008]. Velocity profiles were collected in 2011 and 2012 using a Lowered Acoustic Doppler Current Profiler (LADCP), which were detided using a 1/60° North Atlantic Ocean tidal model (see http://volkov.oce.orst.edu/tides/Ice.html) based on the original model of *Egbert and Erofeeva* [2002]. To compute freshwater fluxes (FWF), absolute geostrophic velocities (V) perpendicular to each section were calculated by referencing the thermal wind shear to the vertically averaged LADCP velocities in the upper 100–500 m for 2011 and 2012. No LADCP data were obtained in 2013; hence, absolute surface geostrophic velocities from Ssalto/Duacs gridded Mean Absolute Dynamic Topography (MADT) were used to reference the thermal wind shear. All S and V data were interpolated on a grid with 1 km horizontal spacing, 5 m vertical spacing in the upper 150 m, and, below that, on bottom-following contours.

To determine the contributions of source waters, water samples were taken for phosphate (PO_4), nitrate (NO_3), and oxygen isotope ratio ($\delta^{18}O$) at sampling depths of 5, 20, 50, 75, 100, 150, 200, and 300 m. Pacific water (PW) can be distinguished from Atlantic water (AW) because of their distinct NO_3-PO_4 relationship [*Jones et al.*, 1998]. Here we use the same PW source line as *Jones et al.* [2008a] and *Dodd et al.* [2012] (referred to as DO12 hereafter) to determine PO_4^{PW}. The AW source line is also adopted from DO12 in order to determine $PO_4^{AW^*}$ where AW* includes AW, river water, and sea ice meltwater [*Jones et al.*, 2008a, 2008b]. The fraction of PW is then determined according to

$$f_{\mathrm{PW}} = \frac{PO_4^m - PO_4^{AW^*}}{PO_4^{PW} - PO_4^{AW^*}},$$

where subscript m indicates the measured value. Fractions of AW, MW, and SIM are found solving end-member equations for mass, $\delta^{18}O$, and S:

$$f_{\mathrm{AW}} + f_{\mathrm{MW}} + f_{\mathrm{SIM}} = 1 - f_{\mathrm{PW}}$$
$$O^{18}_{\mathrm{AW}} f_{\mathrm{AW}} + O^{18}_{\mathrm{MW}} f_{\mathrm{MW}} + O^{18}_{\mathrm{SIM}} f_{\mathrm{SIM}} = O^{18}_m - O^{18}_{\mathrm{PW}} f_{\mathrm{PW}}$$
$$S_{\mathrm{AW}} f_{\mathrm{AW}} + S_{\mathrm{MW}} f_{\mathrm{MW}} + S_{\mathrm{SIM}} f_{\mathrm{SIM}} = S_m - S_{\mathrm{PW}} f_{\mathrm{PW}},$$

with end-member values for $\delta^{18}O$ chosen as $O^{18}_{\mathrm{AW}} = 0.35‰$, $O^{18}_{\mathrm{MW}} = -18.4‰$, $O^{18}_{\mathrm{SIM}} = +0.5‰$, and $O^{18}_{\mathrm{PW}} = -1.3‰$ and for salinity $S_{\mathrm{AW}} = 34.9$, $S_{\mathrm{MW}} = 0$, $S_{\mathrm{SIM}} = 4$, and $S_{\mathrm{PW}} = 32.0$. These values follow DO12 with the exception that we adopted our observed value of O^{18}_{AW} which was on average 0.05‰ larger than DO12. If the lower end-member of DO12 was used, positive netSIM values at 200 m depth were obtained, which is nonphysical.

Since PW and SIM have a salinity value distinct from zero, their contributions to the freshwater are determined as Pacific freshwater $\mathrm{PFW} = f_{\mathrm{PW}} \cdot (S_{\mathrm{AW}} - S_{\mathrm{PW}})/S_{\mathrm{AW}}$ and the net fraction of SIM $\mathrm{netSIM} = f_{\mathrm{SIM}} \cdot$

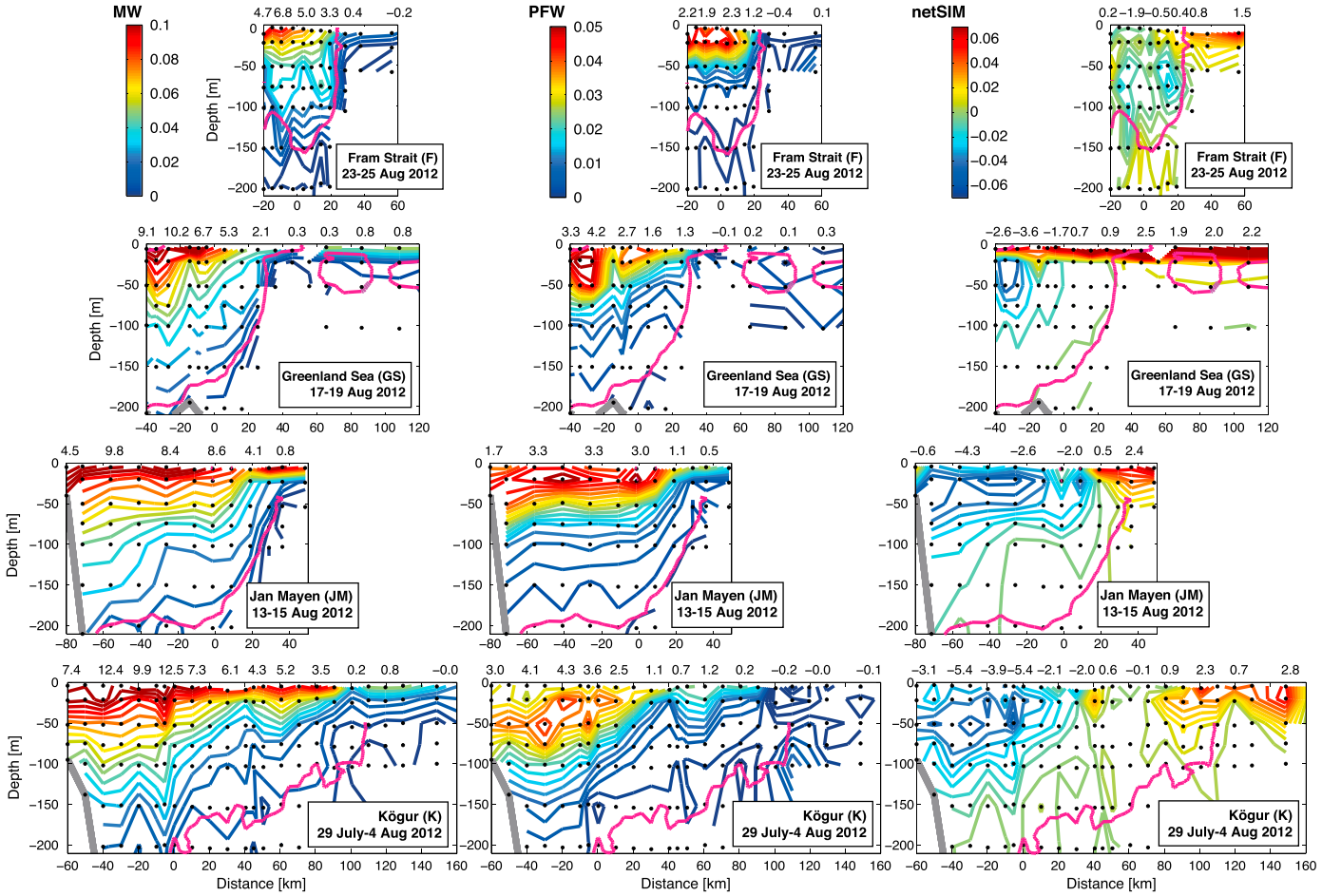

Figure 2. Freshwater fractions of (left column) MW, (middle column) PFW, and (right column) netSIM on sections F, GS, JM, and K going from top to bottom. The quantities are plotted relative to the shelf break at 0 km distance on each section. The black dots show sampling locations. Above each section the vertically integrated value of the inventory is given in meters. The EGPF is indicated with the 0.5° isotherm (magenta line) but is only shown below 50 m on sections JM and K because of the presence of a warm surface layer.

$(S_{AW} - S_{SIM})/S_{AW}$, while MW = f_{MW}. The largest uncertainties in these fractions are associated with the choice of the PW source line. Following either *Jones et al.* [2008a] or *Jones et al.* [1998] leads to differences of 15% in PFW. Second, the error in O^{18}_{MW} results in differences up to 11% in MW. The column freshwater inventories were determined on each section by interpolating the fractions on 2 m bins and integrating vertically to the S_{ref} isohaline or to the bottom of the shelf when S_{ref} was not present. We also calculated the Pacific freshwater inventory using the end-member values used by *Sutherland et al.* [2009] (referred to as SU09) to compare our results with earlier estimates of PFW.

3. Results

Vertical sections of freshwater fractions of MW, PFW, and netSIM are shown for the four transects occupied in 2012 (Figure 2). Distances along each section are relative to the shelf break (at 0 km). In addition, the 0.5° isotherm is added in magenta to highlight the East Greenland Polar Front (EGPF) which marks the seaward boundary of the EGC. Note that only the two southern sections, JM and K, spanned the entire shelf (Figure 1), while the two northern sections, GS and F, covered only 40% and less than 10% of the shelf, respectively.

The largest FW constituent on all of the sections was MW, with fractions up to 0.1. Progressing southward from Fram Strait to Kögur, MW becomes larger and extends deeper from 50 m at section F to 100 m at section K. Small amounts of MW were also present east of the EGPF in contrast to PFW which was mostly confined to the low-salinity waters on the shelf and upper slope. The core of PFW becomes weaker to the

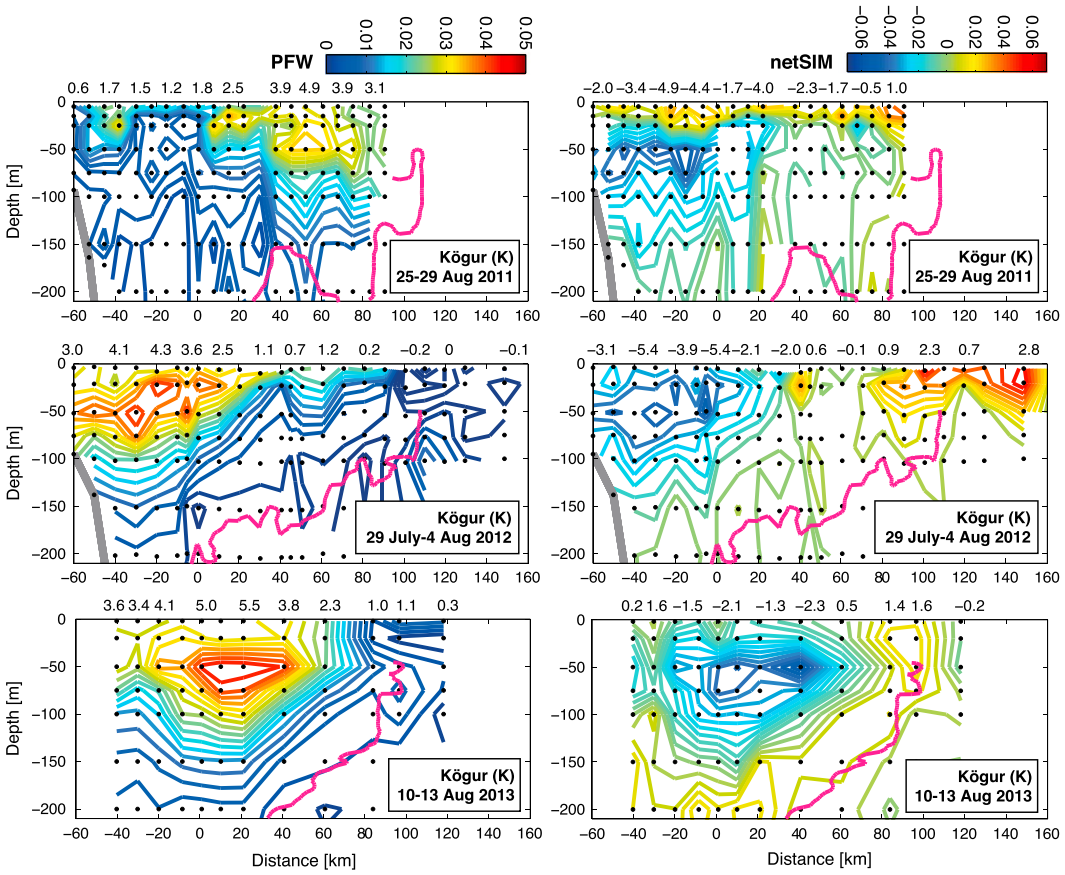

Figure 3. As in Figure 2 but for freshwater fractions of (left column) PFW and (right column) netSIM on section K in (top row) 2011, (middle row) 2012, and (bottom row) 2013.

south and is found at greater depths, particularly on section K. NetSIM had a different distribution. Namely, distinct positive values were observed mostly seaward of the EGPF in the upper 50 m on all four sections and also on the shelf at section GS in a thin (20 m thick) layer. Increasingly negative netSIM, i.e., brine originating from freezing, was seen on the shelf progressing equatorward from section GS to section K (reaching 120 m depth on section K). Tracer data were also obtained at the Kögur section in 2011 (between the Greenland coast to the Iceland slope; −60 to 90 km) and in 2013 (from the inner Greenland shelf to higher up the Iceland slope; −40 to 120 km) (Figure 3). This shows that the distributions of PFW and netSIM are highly variable. For instance, PFW is present much farther east in 2011 and is visible as a strong core over the slope in 2013 and netSIM is positive near the surface across the entire section in 2011.

The water column FW inventory (i.e., the vertical integral) and its components—MW, PFW, and netSIM—were computed for the four sections in 2012 (Figure 4, left column). (The nearshore regions on sections JM and K are excluded because the inventories there are biased low due to the shallow shelf.) The largest freshwater contribution on all four sections was from MW which was largest inshore of the shelf break and increasing going south. For section JM, the FW curve was extended eastward beyond the region of water samples using the CTD data (dashed red line). This shows a small second peak in FW 90 km east of the shelf break. PFW was the second largest contributor, also with maxima on the shelf and nearly zero contribution east of the EGPF. Negative netSIM (brine) dominates on the shelf, while netSIM accumulated up to +2 m on the eastern end of the sections.

The inventories for section K are compared for 2011–2013 (Figure 4, right column). Since CTD measurements were taken farther east, the total FWC up to the Iceland shelf break could be included (dashed lines in Figure 4, top right). There are significant differences between the years. In 2011 the total freshwater and MW inventories were particularly large on the Greenland shelf. In addition, there was a second peak in FWC at ~80 km. Another offshore peak in freshwater content was present in 2013 closer to Iceland. While maximum

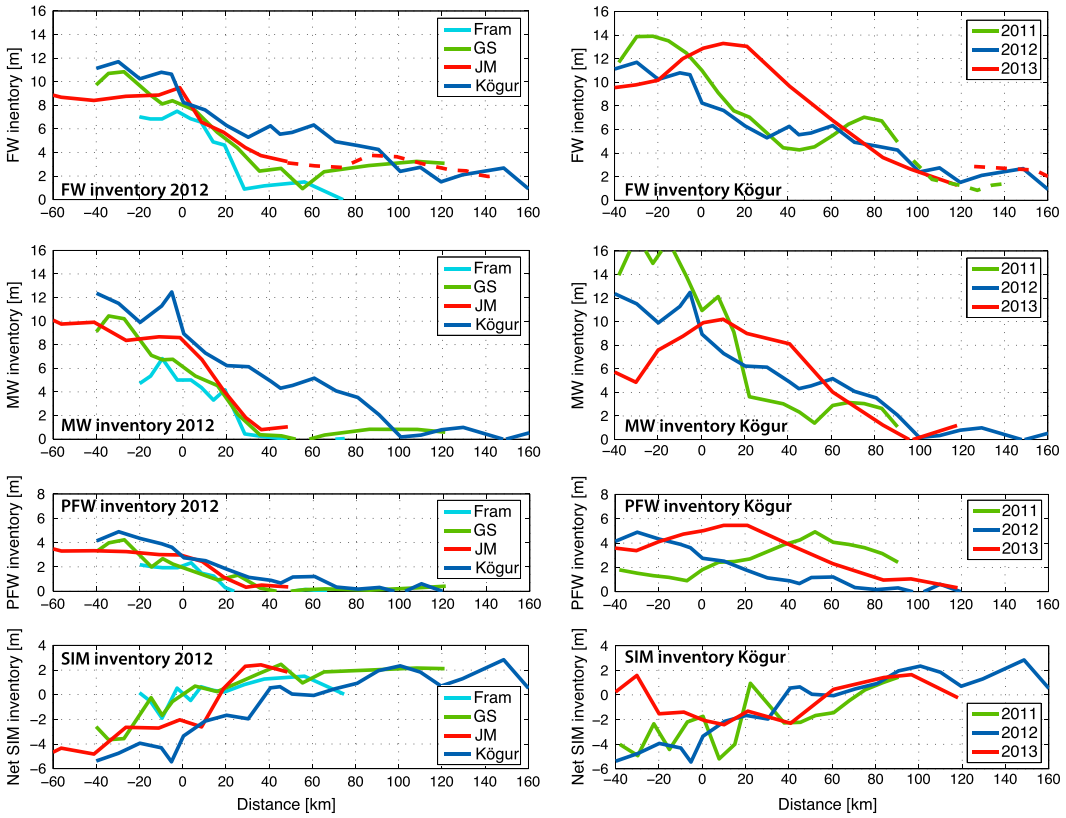

Figure 4. (left column) Column inventories of FW, MW, PFW, and netSIM of the sections F, GS, JM, and K in 2012. (right column) Column inventories of FW, MW, PFW, and netSIM on just the Kögur section in 2011, 2012, and 2013. All inventories are plotted relative to the shelf break at 0 km distance on each section.

PFW was present on the shelf in 2012, in 2013 it was located near the shelf break (10–20 km), and in 2011 it was even farther offshore (50 km). Negative netSIM (large brine content) was observed on the shelf in 2011 and 2012. Maximum netSIM occurred mostly on the eastern end of the EGPF and east of that in all 3 years. In 2013, however, there was more positive SIM present in the near-surface layer across the entire section leading to a secondary maximum of netSIM on the shelf at −30 km distance.

The section-mean inventories for 2011, 2012, and 2013 on the Kögur section were determined by integrating between −40 km and 90 km, i.e., where data existed in all 3 years (Figure 5a). The maximum in total freshwater occurred in 2013, yet the MW signal was lowest that year. Notably, both the PFW and netSIM constituents were largest in 2013. In fact, netSIM was zero in 2013, suggesting that brine was fully compensated by positive SIM in 2013, in contrast to the other 2 years when brine still dominated over SIM. The freshwater fluxes integrated over the same distance are shown in Figure 5b given in mSv (1 mSv = 10^3 $m^{3/s}$, and negative = southward flux). The net flux was −105 ± 22 mSv in 2011, −81 ± 18 mSv in 2012, and −104 ± 41 mSv in 2013. Since there were no LADCP data in 2013, root-mean-square errors obtained from the difference between thermal wind shear at the surface and absolute surface geostrophic velocities obtained from MADT in 2013 lead to a larger error estimate. We note that the fluxes of FW and MW varied similarly as the inventories, but this was not the case for the flux of netSIM. Even though the normalized netSIM on the section was zero, a net positive flux of netSIM was found in 2013 since the minimum netSIM (brine (negative)) was found in the (southward (negative)) core of the EGC. The flux of PW was largest in 2013 and made up one third to the total FWF.

The normalized amount of PFW (in meters) between −60 km (the coast) and 90 km on the Kögur section was determined following SU09 who quantified PFW over that same 150 km distance on this section. (Inventories in 2013 were extrapolated to the coast assuming a similar distribution at −60 km relative to −40 km as in earlier years.) The calculation was done based on our choice of end-members, as well as for the end-members used by SU09 (Figure 5c). Results for the late-1990s and 2000s adopted from SU09 are

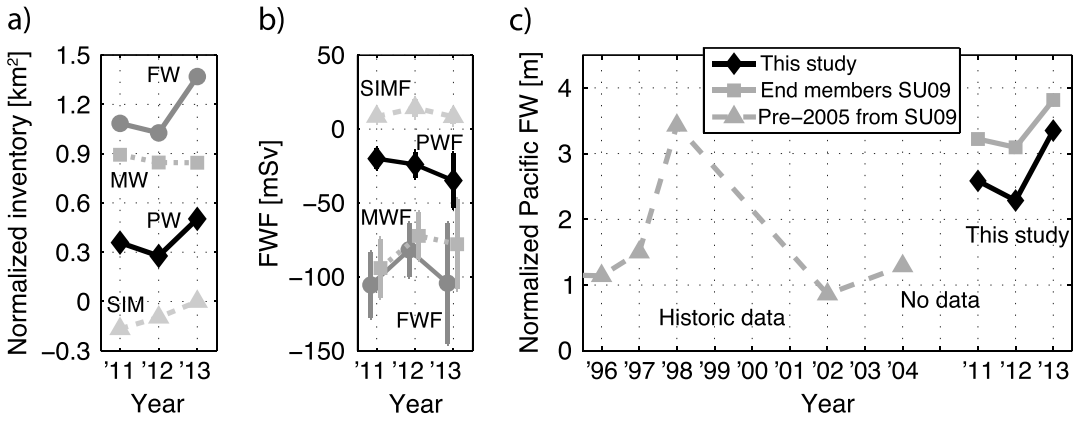

Figure 5. (a) Integrated inventories of FW, MW, PFW, and netSIM calculated between −40 km and 90 km distance on section K for 2011, 2012, and 2013 and (b) net fluxes of the inventories on section K integrated over the same distance. (c) Normalized Pacific freshwater in meters between −60 km and 90 km distance with end-members used in this study, with end-members of SU09, and pre-2005 data from SU09.

also included. For the years considered here, using the end-members based on our study, there were large amounts of PFW with a section-mean value varying from 2.3 to 3.3 m (black line/diamonds). These represent a lower bound of PFW, while the end-members of SU09 result in larger values up to 3.8 m (gray line/squares). Regardless of the end-members used, the PFW on the Kögur section in recent years is larger compared to earlier data, and in 2013 the PFW value is comparable to the previous maximum in 1998.

4. Discussion

In the data presented here, collected between 2011 and 2013, the largest contributor to the FWC on the shelf and in core of the EGC west of the EGPF was MW, followed by a significant amount of PFW in all 3 years. We note that the complete FWC across the shelf was captured only on the southern two sections JM and K. Between these two transects the integrated inventories show a small increase in total FWC and MW, which can be attributed to runoff from Greenland. The lateral distribution of PFW on the Kögur section was most variable between the occupations. In 2011 PFW dominated the FWC seaward of the shelf break while still being inshore of the EGPF. The reason for this eastward shift in 2011 is unclear, but it may be due to the sporadic occurrence of eddies spawned from the EGC farther upstream [*Våge et al.*, 2013]. Such a turbulent flux may be an effective mechanism for removing FW from the shelf break EGC in this area.

Near the EGPF and seaward of this—in the Greenland and Iceland seas—the FWC was dominated by SIM as far north as Fram Strait. Since PFW and negative netSIM (a surplus of brine) are not seen east of the EGPF on sections F, GS, and K, we assume that the FWC east of 50 km distance on section JM also consists of SIM. Under this assumption there is a small increase in total SIM between sections JM and K progressing southward. However, this is not associated with an increase in netSIM flux at section K. On the contrary, the maximum SIM on that section occurs in the northward flowing NIIC located east of 140 km. This leads to a northward transport of 11 $\pm$ 2.4 mSv of SIM here, while the transport of MW and PFW are 2 $\pm$ 0.44 mSv and 0.5 $\pm$ 0.12 mSv, respectively. From these observations in 2012 we surmise that sea ice is more easily lost from the EGC into the Nordic Seas, where it subsequently melts in summer as it meets warmer waters. There appears to be hardly any loss of the liquid components of FW into the Nordic Seas, which is in agreement with results of *Dodd et al.* [2009].

The large amounts of PFW observed here suggest a change in the pathway of this water toward Fram Strait and likely a temporal release of FW from the Arctic. The presence of large amounts of PFW in 2011 is consistent with DO12, who showed that PFW was first observed again in Fram Strait in 2011, which was preceded by a freshwater anomaly in the Lincoln Sea between 2007 and 2010 [*de Steur et al.*, 2013]. The PFW value measured in 2013 on the Kögur section is as large as the previous maximum observed in 1998 (SU12). Despite the large gap in observations between 2004 and 2011 near Denmark Strait, and the fact that the occurrence of Pacific water in the EGC is intermittent [*Taylor et al.*, 2003], we surmise that the PFW over that time period was small, considering the fact that it was not observed in Fram Strait (DO12).

While large amounts of PFW were observed during all three occupations of the Kögur section—with a maximum in 2013—we found that the MW inventory decreased and that netSIM increased due to a reduction in brine. These observations imply a slightly weaker contribution of Siberian shelf water to the EGC during recent years and an increased contribution from Canadian Basin freshwater. This is consistent with significant changes in PFW that have occurred in the Pacific Arctic during the last decade. In particular, the influx of Pacific water through Bering Strait increased since 2001, with a high record in 2011 [*Woodgate et al.*, 2012], while the eastward flux of PFW in the Beaufort shelf break jet has diminished over the same time period due to enhanced easterly winds [*Brugler et al.*, 2014]. As such, more PFW has been available to enter the Beaufort Gyre and extend farther north into the Canadian Basin, providing a shorter pathway to Fram Strait. This suggests that the combination of enhanced Pacific water inflow and a change in the pathway of PFW into the central Arctic likely caused the recent large amounts of PFW near Denmark Strait documented here.

Acknowledgments

The research leading to these results has received funding from the European Union Seventh Framework Programme (FP7 2007–2013) under grant agreement 308299, NACLIM Project, and from the U.S. National Science Foundation under grant OCE-085041. The altimeter products were produced by Ssalto/Duacs and distributed by Aviso, with support from CNES (http://www.aviso.oceanobs.com/duacs/). We would like to thank the crew of the R/V *Knorr*, the RSS *James Clark Ross*, and the R/V *Bjarni Sæmundsson*, as well as the technicians and students who contributed to the data collection.

The Editor thanks two anonymous reviewers for their assistance in evaluating this paper.

References

Aagaard, K., J. H. Swift, and E. C. Carmack (1985), Thermohaline circulation in the Arctic Mediterranean Seas, *J. Geophys. Res.*, *90*(C3), 4833–4846.

Bauch, D., P. Schlosser, and R. G. Fairbanks (1995), Freshwater balance and the sources of deep and bottom waters in the Arctic Ocean inferred from the distribution of $H_2{}^{18}O$, *Prog. Oceanog.*, *35*, 53–80.

Brugler, E. T., R. S. Pickart, G. W. K. Moore, S. Roberts, T. J. Weingartner, and H. Statscewich (2014), Seasonal to interannual variability of the Pacific water boundary current in the Beaufort Sea, *Prog. Oceanogr.*, *127*, 1–20, doi:10.1016/j.pocean.2014.05.002.

de Steur, L., et al. (2013), Hydrographic changes in the Lincoln Sea in the Arctic Ocean with focus on an upper ocean freshwater anomaly between 2007 and 2010, *J. Geophys. Res. Oceans*, *118*, 4699–4715, doi:10.1002/jgrc.20341.

Dickson, R. R., B. Rudels, S. Dye, M. Karcher, J. Meincke, and I. Yashayaev (2007), Current estimates of freshwater flux through Arctic and subarctic seas, *Prog. Oceanogr.*, *73*, 210–230.

Dodd, P. A., K. J. Heywood, M. P. Meredith, A. C. Naveira-Garabato, A. D. Marca, and K. K. Falkner (2009), Sources and fate of freshwater exported in the East Greenland Current, *Geophys. Res. Lett.*, *36*, L19608, doi:10.1029/2009GL039663.

Dodd, P. A., B. Rabe, E. Hansen, E. Falck, A. Mackensen, E. Rohling, C. Stedmon, and S. Kristiansen (2012), The freshwater composition of the Fram Strait outflow derived from a decade of tracer measurements, *J. Geophys. Res.*, *117*, C11005, doi:10.1029/2012JC008011.

Egbert, G. D., and S. Erofeeva (2002), Efficient inverse modeling of barotropic ocean tides, *J. Atmos. Oceanic Technol.*, *19*(2), 83–204.

Falck, E., G. Kattner, and G. Budéus (2005), Disappearance of Pacific water in the northwestern Fram Strait, *Geophys. Res. Lett.*, *32*, L14619, doi:10.1029/2005GL023400.

Giles, K. A., S. W. Laxon, A. L. Ridout, D. J. Wingham, and S. Bacon (2012), Western Arctic Ocean freshwater storage increased by wind-driven spin-up of the Beaufort Gyre, *Nat. Geosci.*, doi:10.1038/NGEO1379.

Hansen, E., S. Gerland, M. A. Granskog, O. Pavlova, A. H. H. Renner, J. Haapala, T. B. Løyning, and M. Tschudi (2013), Thinning of Arctic sea ice observed in Fram Strait: 1990–2011, *J. Geophys. Res. Oceans*, *118*, 5202–5221, doi:10.1002/jgrc.20393.

Holfort, J., E. Hansen, S. Østerhus, S. Dye, S. Jonsson, J. Meincke, J. Mortensen, and M. Meredith (2008), Freshwater fluxes east of Greenland, in *Arctic-Subarctic Ocean fluxes*, edited by R. R. Dickson, J. Meincke, and P. Rhines, pp. 263–288, Springer, Netherlands.

Jones, E. P., L. G. Anderson, and J. H. Swift (1998), Distribution of Atlantic and Pacific waters in the upper Arctic Ocean: Implications for circulation, *Geophys. Res. Lett.*, *25*(6), 765–768, doi:10.1029/98GL00464.

Jones, E. P., L. G. Anderson, S. Jutterström, L. Mintrop, and J. H. Swift (2008a), Pacific freshwater, river water and sea ice meltwater across Arctic Ocean basins: Results from the 2005 Beringia Expedition, *J. Geophys. Res.*, *113*, C08012, doi:10.1029/2007JC004124.

Jones, E. P., L. G. Anderson, S. Jutterström, and J. H. Swift (2008b), Sources and distribution of fresh water in the East Greenland Current, *Prog. Oceanogr.*, *78*, 37–44, doi:10.1016/j.pocean.2007.06.003.

Morison, J., R. Kwok, C. P. Peralta-Ferritz, M. Alkire, I. Rigor, R. Andersen, and M. Steele (2012), Changing Arctic Ocean freshwater pathways, *Nature*, *481*, 66–70, doi:10.1038/nature10705.

Perovich, D., W. Meier, M. Tschudi, S. Gerland, and J. Richter-Menge (2012), Sea ice, in *Arctic Report Card 2012*, edited by M. O. Jeffries, J. A. Richter-Menge, and J. E. Overland, pp. 37–42. [Available at http://www.arctic.noaa.gov/report12/ArcticReportCard_full_report.pdf.]

Proshutinsky, A., R. Krishfield, M.-L. Timmermans, J. Toole, E. Carmack, F. A. McLaughlin, W. J. Williams, S. Zimmerman, M. Itoh, and K. Shimada (2009), The Beaufort Gyre freshwater reservoir: State and variability from observations, *J. Geophys. Res.*, *114*, C00A10, doi:10.1029/2008JC005104.

Rabe, B., M. Karcher, U. Schauer, J. Toole, R. A. Krishfield, S. Pisarev, F. Kauker, R. Gerdes, and T. Kikuchi (2011), An assessment of pan-Arctic Ocean freshwater content changes from the 1990s to the IPY period, *Deep Sea Res. Part I*, *58*, 173–185, doi:10.1016/j.dsr.2012.12.002.

Serreze, M. C., A. P. Barrett, A. G. Slater, R. A. Woodgate, K. Aagaard, R. B. Lammers, M. Steele, R. Moritz, M. Meredith, and C. M. Lee (2006), The large-scale freshwater cycle of the Arctic, *J. Geophys. Res.*, *111*, C11010, doi:10.1029/2005JC003424.

Steele, M., J. Morison, W. Ermold, I. Rigor, M. Ortmeyer, and K. Shimada (2004), Circulation of summer Pacific halocline water in the Arctic ocean, *J. Geophys. Res.*, *109*, C02027, doi:10.1029/2003JC002009.

Sutherland, D. A., R. S. Pickart, E. P. Jones, K. Azetsu-Scott, A. J. Eert, and J. Ólafsson (2009), Freshwater composition of the waters off southeast Greenland and their link to the Arctic Ocean, *J. Geophys. Res.*, *114*, C05020, doi:10.1029/2008JC004808.

Taylor, J. R., K. K. Falkner, U. Schauer, and M. Meredith (2003), Quantitative considerations of dissolved barium as a tracer in the Arctic Ocean, *J. Geophys. Res.*, *108*(C12), 3374, doi:10.1029/2002JC001635.

Våge, K., R. S. Pickart, M. A. Spall, G. Moore, H. Valdimarsson, D. J. Torres, S. Y. Erofeeva, and J. E. Ø. Nilsen (2013), Revised circulation scheme north of the Denmark Strait, *Deep Sea Res. Part I*, *79*, 20–39, doi:10.1016/j.dsr.2013.05.007.

Woodgate, R. A., T. J. Weingartner, and R. Lindsay (2012), Observed increases in Bering Strait oceanic fluxes from the Pacific to the Arctic from 2001 to 2011 and their impacts on the Arctic Ocean water column, *Geophys. Res. Lett.*, *39*, L24603, doi:10.1029/2012GL054092.